PROCEEDINGS OF SCIENCE

SLAC-PUB-15539

Status of $|V_{ub}|$ and $|V_{cb}|$ determinations

Robert Kowalewski[*†]
University of Victoria
E-mail: kowalews@uvic.ca

The determination of the CKM matrix elements $|V_{ub}|$ and $|V_{cb}|$ is the focus of substantial experimental and theoretical effort. Both exclusive and inclusive semileptonic B decays are used to determine these quantities; these two approaches use complementary theoretical descriptions. The experimental measurements are dominated by results from the e^+e^- B factories. The trend seen in recent years for the determinations based on inclusive decays to give larger values than the determinations based on exclusive decays continues.

Flavor Physics and CP Violation - FPCP 2010
May 25-29, 2010
Turin, Italy

[*]Speaker.
[†]On behalf of the BABAR collaboration.

This material is based upon work supported by the U.S. Department of Energy, Office of Science, Office of Basic Energy Sciences, under Contract No. DE-AC02-76SF00515 and HEP.

1. Semileptonic B decays

The main challenge in determining the CKM matrix elements $|V_{cb}|$ and $|V_{ub}|$ is to reduce the decay rate uncertainties caused by the strong interaction. This leads one to use the semileptonic decays $\bar{B} \to X\ell\bar{\nu}$, which involve only one hadronic current. The presence of a charged lepton in the final state provides a clean experimental signature for these decays, but the presence of a neutrino reduces the kinematic constraints available to distinguish signal from background. Decays to charmed (X_c) and charmless (X_u) hadronic states can be distinguished experimentally primarily via kinematics, since the minimum X_c mass is m_D, and to some extent by the presence of kaons and detached vertices in the final state. The squared momentum transferred to the leptons in the semileptonic decay is denoted by q^2.

The weak decay of a left-handed spin-1/2 fermion is calculable to high precision in the standard model. The impact of strong interaction corrections to this picture (see Fig. 1) can be systematically incorporated using the Operator Product Expansion (OPE)[1]. The OPE is a double expansion in powers of α_S and Λ_{QCD}/m_b, where Λ_{QCD} represents a typical QCD scale of 0.5-1.0 GeV/c^2. Its application to modeling inclusive decays relies on the validity of analytic continuation into the region of time-like momenta ($p_B^2 = M_B^2$), which is equivalent to the assumption of quark-hadron duality. The leading term in the OPE expression for the semileptonic B decay rate reproduces the parton model. Non-perturbative contributions arise as matrix elements of each local operator appearing in the expansion. The first power correction vanishes, leaving terms of order $O(\Lambda_{QCD}^2/m_b^2)$ as the leading corrections.

Exclusive semileptonic decays, where the hadron accompanying the lepton pair is explicitly reconstructed, are described as weak decays with q^2-dependent form factors. The calculation of these form factors requires non-perturbative QCD methods, such as lattice QCD (LQCD) or light-cone sum rules (LCSR). While neither method is able to provide precise value of the full q^2 range, they complement each other, with LQCD best suited to large ($q^2 > 16\,\text{GeV}^2/c^4$) values and LCSR best suited to small ($q^2 < 12\,\text{GeV}^2/c^4$) values.

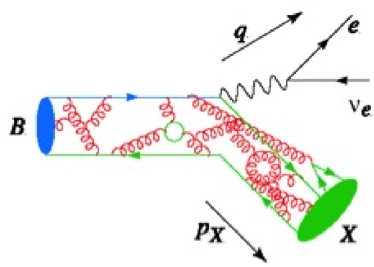

Figure 1: Cartoon of semileptonic B decay

The measurement of inclusive semileptonic B decays starts with an identified electron or muon above some momentum cut, usually about $1\,\text{GeV}/c$ in the B rest frame. The measurement of the electron momentum spectrum requires relatively few additional cuts, primarily to reduce the level of background from continuum $e^+e^- \to q\bar{q}$ events. Analyses wishing to use q^2 must additionally determine the missing momentum vector of the event; the modeling of the resolution in this variable is sensitive to limited acceptance and imperfect reconstruction of *a priori* visible momentum. The use of properties of the accompanying hadronic system, like the hadronic mass m_X, requires an assignment of each particle to one of the two B mesons. This entails fully reconstructing the second B meson in the event, since the decay products of the two B mesons overlap in the detector. This "recoil method", is very powerful, and results in clean samples of semileptonic decays. It does, however, come at a substantial cost; the efficiency for fully reconstructing the second B meson is $\approx 0.3\%$.

Exclusive semileptonic decays are measured by fully reconstructing a hadron (D, D^*, π, ρ, etc.) and requiring the kinematics of the event to be consistent with a semileptonic decay; in particular, that the missing energy and missing momentum are roughly equal. Analyses using fully differential spectra allow the determination of both the decay rate and the slope of the form factor, and of two additional form factor ratios in decays with a vector hadron in the final state. Analyses of $\bar{B} \to X_u \ell \bar{\nu}$ decays reduce background by further requiring the remaining particles in the event to be consistent with a B meson decay, either through full reconstruction, through a somewhat looser criterion in which the second B is reconstructed in a common semileptonic decay ($\varepsilon \approx 0.6\%$) or by making loose requirements on the energy and invariant mass of the set of remaining particles.

2. Exclusive $\bar{B} \to X_c \ell \bar{\nu}$ decays

The differential decay rate for $\bar{B} \to D \ell \bar{\nu}$ is given by[1]

$$\frac{d\Gamma(\bar{B} \to D\ell\bar{\nu})}{dw} = \frac{G_F^2 |V_{cb}|^2}{48\pi^3} \left(\mathscr{G}(w)\right)^2 \Phi(w) \tag{2.1}$$

where $\mathscr{G}(w)$ is the form factor, $\Phi(w)$ is a phase space factor, and

$$w \equiv \frac{m_B^2 + m_D^2 - q^2}{2m_B m_D} \tag{2.2}$$

is the boost of the D meson in the $\bar{B}$ rest frame ($1 < w < 1.59$). The point $w = 1$ corresponds to maximum q^2, where the final state hadron is at rest in the B rest frame. This "zero recoil" point is special in the limit of heavy quark symmetry, and the form factor there is unity: $\lim_{m_b, m_c \to \infty} \mathscr{G}(1) = 1$. Corrections to this limit are parameterized as functions of $w-1$ or in terms of a modified expansion variable

$$z \equiv \frac{\sqrt{w+1} - \sqrt{2}}{\sqrt{w+1} + \sqrt{2}}; \qquad 0 < z < 0.065. \tag{2.3}$$

Unitarity and analyticity can be used to constrain the expansion coefficients. The differential decay rate for $\bar{B} \to D^* \ell \bar{\nu}$ is similar, but there are three independent form factors in the decay (denoted below by A_1, A_2 and V), and the differential rate depends on three angles in addition to w (or z).

2.1 $\bar{B} \to D^* \ell \bar{\nu}$

Measurements of $\bar{B} \to D^* \ell \bar{\nu}$ decays have been made at CLEO, LEP and the B factories. Recent measurements have significantly better precision and are based on three different methods. All

[1] Setting lepton masses to zero.

measurements of $\bar{B}^0 \to D^{*+}\ell\bar{\nu}$[2, 3] and $B^- \to D^{*0}\ell\bar{\nu}$[4, 5] determine the branching fraction, the form factor slope at zero recoil (ρ^2_{A1}) and the product $\mathscr{F}(1)|V_{cb}|$. In addition, some analyses[2] of $\bar{B}^0 \to D^{*+}\ell\bar{\nu}$ also measure the form factor ratios $R_1 = A_2/A_1$ and $R_2 = V/A_1$ at $w = 1$. Measurement of the $B^- \to D^{*0}\ell\bar{\nu}$ mode provides a valuable experimental cross-check, as the systematic uncertainty associated with the transition pion reconstruction in the $D^* \to D\pi$ decay is different than in the D^{*+} case. A global analysis[5] of $\bar{B} \to DX\ell\bar{\nu}$ based on the kinematic properties of the D-ℓ pair is completely independent of soft pion reconstruction. In all analyses the limiting experimental uncertainties are from detector modeling (particle reconstruction and identification efficiencies), background from the $\approx 15\%$ of the $\bar{B} \to X_c\ell\bar{\nu}$ rate that is poorly understood, and, where not directly measured, uncertainties in R_1 and R_2. The theoretical uncertainty on the form factor normalization $\mathscr{F}(1)$ is dominant in determinations of $|V_{cb}|$.

The HFAG averages[6] (see Fig. 2) are

$$\mathscr{F}(1)|V_{cb}| = (35.5 \pm 0.5) \times 10^{-3} \tag{2.4}$$
$$\rho^2_{A1} = 1.16 \pm 0.05 \tag{2.5}$$

Our determination of $|V_{cb}|$ uses an unquenched LQCD result,[7] $\mathscr{F}(1) = 0.927 \pm 0.013 \pm 0.020$, and scales the error on the average by $\sqrt{\chi^2/\mathrm{ndf}} = 1.37$ to find

$$|V_{cb}|_{D^*} = (38.3 \pm 0.7_{\mathrm{exp}} \pm 1.0_{\mathrm{th}}) \times 10^{-3} \tag{2.6}$$

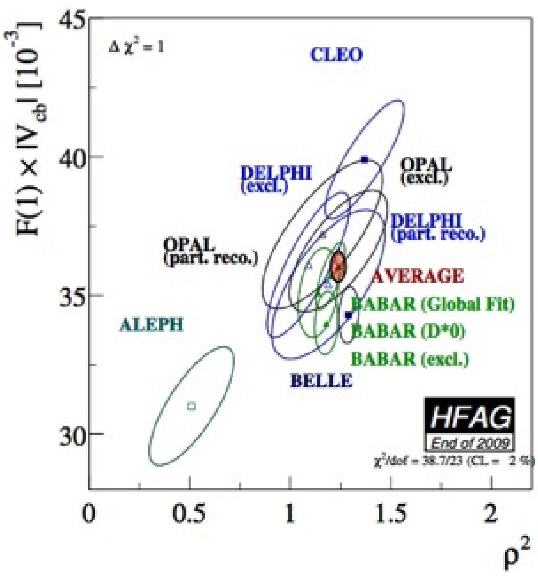

Figure 2: Measurements of $\mathscr{F}(1)|V_{cb}|$ versus ρ^2_{A1} compiled by HFAG.

2.2 $\bar{B} \to D\ell\bar{\nu}$

The decay $\bar{B} \to D\ell\bar{\nu}$ provides a second avenue for determining $|V_{cb}|$ in exclusive decays. The decay is easier to implement on the lattice than $\bar{B} \to D^*\ell\bar{\nu}$, although existing calculations are not yet at the same level of accuracy. Experimentally, the presence of feed-down from $\bar{B} \to D^* \ell \bar{\nu}$ decays makes this mode more challenging. Two recent BABAR results[5, 8] have significantly improved the experimental picture. The main experimental uncertainties come again from detector modeling and $\bar{B} \to X_c \ell \bar{\nu}$ backgrounds. Use of the full B factory data samples could reduce the experimental uncertainty by a factor of about 0.8.

The HFAG averages[6] are

$$\mathscr{G}(1)|V_{cb}| = (42.3 \pm 1.5) \times 10^{-3} \tag{2.7}$$

$$\rho^2 = 1.18 \pm 0.06 \tag{2.8}$$

Using $\mathscr{G}(1) = 1.074 \pm 0.018 \pm 0.016$ from a preliminary unquenched LQCD calculation[9] gives

$$|V_{cb}|_D = (39.1 \pm 1.4_{\rm exp} \pm 1.3_{\rm th}) \times 10^{-3} \tag{2.9}$$

where the lattice errors have been added linearly. Both the slope and the $|V_{cb}|$ values agree well with those obtained from $\bar{B} \to D^* \ell \nu$ decays. Given the improved experimental accuracy, more precise determinations of $\mathscr{G}(1)$ will be helpful.

3. Inclusive $b \to c \ell \bar{\nu}$ decays

The OPE expression for the semileptonic decay width is (schematically)

$$\Gamma(b \to c \ell \bar{\nu}) = \frac{G_F^2 m_b^5}{192\pi^3} |V_{cb}|^2 (1 + A_{ew}) A^{pert}(r, \mu) \left[z_0(r) + z_2(r) \left(\frac{\mu_\pi^2}{m_b^2}, \frac{\mu_G^2}{m_b^2} \right) + z_3(r) \left(\frac{\rho_D^3}{m_b^3}, \frac{\rho_{LS}^3}{m_b^3} \right) + \ldots \right] \tag{3.1}$$

where $r = m_c/m_b$, A_{ew} and A^{pert} are electroweak and perturbative QCD corrections, and the non-perturbative quantities μ_π^2, μ_G^2, ρ_D^3 and ρ_{LS}^3 are matrix elements of local operators whose values are to be determined from data. These same non-perturbative quantities appear in calculated moments of the spectrum for decays satisfying $E_\ell > E_0$:

$$\langle E_\ell^n M_X^{2m} \rangle_{E_0} = \frac{1}{\Gamma_0} \int_{E_0}^{E_{max}} dE_\ell \int dM_X^2 \frac{d\Gamma(\mu_\pi^2, \mu_G^2, \rho_D^3, \ldots)}{dE_\ell dM_X^2} E_\ell^n M_X^{2m} \tag{3.2}$$

This allows one to measure a large number of experimental moments in the electron energy or hadronic mass or energy, for a variety of minimum lepton energy thresholds, and perform a global fit to extract $|V_{cb}|$, m_b and m_c, and the non-perturbative parameters in the expression. Perturbative corrections[10] are known to α_S^2 on leading terms and α_S on $1/m_b$ terms, although not all corrections are incorporated into global fits using these moments. The calculations are available in two mass renormalization schemes: the "1S" scheme[11] and the "kinetic" scheme[12]. Similar expansions can be written for $b \to u \ell \bar{\nu}$ and $b \to s\gamma$ decays.

Experiments at the $\Upsilon(4S)$, CDF and DELPHI have measured spectral moments in $b \to c \ell \bar{\nu}$ decays. Moments of the electron energy spectrum[13] can be measured using inclusive analyses, but moments involving hadronic variables[14] (e.g. m_x^2) require reconstruction of the full semileptonic decay. The uncertainties come principally from detector modeling and the modeling of B and D decays. Measurements of the photon energy moments from $b \to s\gamma$ decays[15] are still statistically limited due to the large background subtraction needed at energies below $\sim 2.2\,\text{GeV}$. A global fit to 64 moments in the kinetic scheme[16] gives the results shown in Table 1. A fit excluding the $b \to s\gamma$ moments gives similar precision on $|V_{cb}|$, but has less sensitivity to m_b. The points used in the fit are correlated - each moment is used at a series of minimum lepton momentum or minimum photon energy cuts, so the samples have significant overlap. These correlations, as well as correlations in the systematic uncertainties, are taken into account in the fit. The treatment of correlations in the theoretical uncertainties (due to, e.g., uncalculated higher order terms, or assumptions on parameters that cannot be determined directly in the fit) is also considered. Nevertheless, the chisquare probability of the fit – 0.9995 – is far too good and demands an explanation.

The results of a global fit in the 1S scheme[17] are similar and give $|V_{cb}| = (41.87 \pm 0.25 \pm 0.08) \times 10^{-3}$, and again give an unreasonably small χ^2/ndf.

Table 1: Global fit results in the kinetic scheme.

Input	$\lvert V_{cb}\rvert(10^{-3})$	m_b^{kin} (GeV)	μ_π^2 (GeV^2)	χ^2/ndf
all moments	$41.54 \pm 0.43_{\text{fit}} \pm 0.08_{\tau_B} \pm 0.58_{\text{th}}$	4.620 ± 0.035	0.424 ± 0.042	$26.4/(64-7)$
only $b \to c\ell\nu$	$41.31 \pm 0.49_{\text{fit}} \pm 0.08_{\tau_B} \pm 0.58_{\text{th}}$	4.678 ± 0.051	0.410 ± 0.046	$20.3/(53-7)$

The $|V_{cb}|$ from the global fit is about 2.4σ higher than the values obtained from $\bar{B} \to D^*\ell\bar{\nu}$ and $\bar{B} \to D\ell\bar{\nu}$ decays. The average of the three values, after scaling the error by $\sqrt{\chi^2/\text{ndf}}$, is

$$|V_{cb}| = (40.6 \pm 1.0) \times 10^{-3} \tag{3.3}$$

4. Inclusive $b \to u\ell\bar{\nu}$ decays

The OPE used to describe $b \to c\ell\bar{\nu}$ decays is valid for $b \to u\ell\bar{\nu}$ decays when calculating quantities over broad regions of phase space. However, the large difference in rate ($b \to c\ell\bar{\nu}$ decays are 50 times more prevelant than $b \to u\ell\bar{\nu}$ decays) makes it experimentally challenging to measure $b \to u\ell\bar{\nu}$ decays in regions where $b \to c\ell\bar{\nu}$ decays are not highly suppressed. The imposition of restrictive kinematic cuts ruins the convergence of the OPE, and brings in dependence on a non-perturbative shape function. In addition, decay rates in restricted regions of phase space depend parametrically on powers of m_b much higher than the m_b^5 of the total semileptonic rate. The presence of competing processes like weak annihilation, which can contribute significantly at high q^2, brings additional uncertainty. Determinations of $|V_{ub}|$ using inclusive decays therefore involve a tradeoff between statistics, experimental systematic uncertainties and theoretical uncertainties.

Measurements of $b \to u\ell\bar{\nu}$ partial rates fall into two broad categories: fully inclusive analyses, where the lepton momentum and, in some cases, the missing (neutrino) momentum are measured; and recoil analyses, where the other B meson in the event is fully reconstructed, allowing a clear identification of the remaining particles with the semileptonically decaying B, and giving access to the full set of potential kinematic variables. The second approach is more flexible and provides some additional background suppression, but suffers from low efficiency. In both approaches, feeddown from mis-reconstructed $b \to c\ell\bar{\nu}$ decays, due to additional neutrinos, limited acceptance

PoS(FPCP 2010)028

and hard-to-reconstruct particles like K_L^0, are significant sources of systematic uncertainty. Other significant sources of uncertainty include detector modeling and the modeling of charm decays.

A recent result from Belle uses a multivariate discriminator to extract the $b \to u\ell\bar{\nu}$ rate with minimal kinematic cuts, namely $E_e > 1\,\mathrm{GeV}$. In this and other analyses that probe deep into the region dominated by $b \to c\ell\bar{\nu}$ decays, the knowledge of the shape of the $b \to u\ell\bar{\nu}$ differential spectrum becomes an important source of systematic uncertainty, and correlations between this uncertainty and theoretical and parametric (m_b) uncertainties are not easy to evaluate. The partial rate measurements used by HFAG are shown in Table 2. These partial rates explore a range of different kinematic regions, providing tests of theoretical partial rate predictions.

Table 2: Partial branching fraction measurements ($\times 10^5$). The total $b \to u\ell\bar{\nu}$ branching fraction in these units is ≈ 220. The entries to the right of the vertical bar are from recoil analyses.

CLEO[18]	BaBar[19]	Belle[20]	BaBar[21]	Belle[22]	BaBar[23]	BaBar[23]	BaBar[23]	Belle[24]
$E_e > 2.1$	E_e-q^2	$E_e > 1.9$	$E_e > 2.0$	m_X-q^2	$m_X < 1.55$	m_X-q^2	P_+	$E_e > 1$
$33 \pm 2 \pm 7$	$44 \pm 4 \pm 4$	$85 \pm 4 \pm 15$	$57 \pm 4 \pm 7$	$74 \pm 9 \pm 13$	$118 \pm 9 \pm 7$	$81 \pm 8 \pm 7$	$95 \pm 10 \pm 8$	$196 \pm 17 \pm 16$

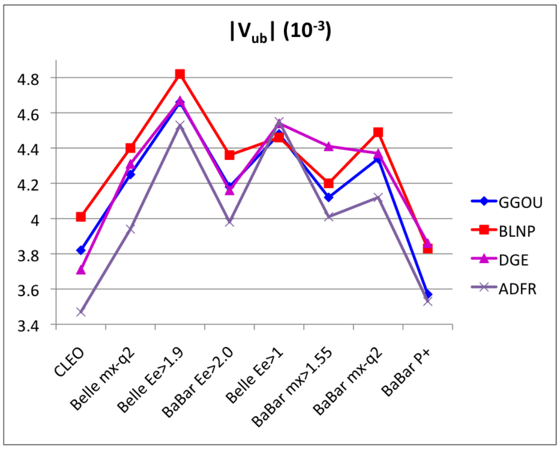

Figure 3: $|V_{ub}|$ determinations from measured $b \to u\ell\bar{\nu}$ partial rates using four different theoretical calculations.

There are several theoretical calculations of these partial rates in terms of $|V_{ub}|^2$; details are in the talk of T. Mannel. They include sophisticated error analyses, including terms for uncertainties from parametric and perturbative sources, weak annihilation and the shape function. The $|V_{ub}|$ determinations based on these calculations are shown in Fig. 3. The spread in $|V_{ub}|$ values for each measurement is roughly consistent with the independent uncertainties assigned in the calculations. Averaging over the partial rates and performing an "average of the averages" gives

$$|V_{ub}| = (4.37 \pm 0.16_{\mathrm{exp}} \pm 0.20_{\mathrm{th}} \pm 0.30_{\mathrm{NNLO}}) \times 10^{-3} \tag{4.1}$$

The last uncertainty has been added "by hand" to account for the larger than expected shift seen in the BLNP calculation[25] (+8% on $|V_{ub}|$; not applied in values quoted here) when NNLO perturbative terms are included. It will be interesting to see whether or not the other calculations see large effects at NNLO.

5. Exclusive $\bar{B} \to X_u \ell \bar{\nu}$ decays

The cleanest exclusive $\bar{B} \to X_u \ell \bar{\nu}$ mode to measure is $\bar{B} \to \pi \ell \bar{\nu}$. This is also, by far, the mode for which theoretical calculations of the decay form factor are most precise. While the program of measuring other charmless exclusive semileptonic B decays is of interest in its own right, for the determination of $|V_{ub}|$ we restrict ourselves to this golden mode.

Here again, measurements are performed both with and without reconstruction of the recoiling B meson. Given the small branching fraction for $\bar{B} \to \pi \ell \bar{\nu}$, the recoil-based measurements[26, 27] are statistically limited, and are unable at present to provide much information on the shape of the partial branching fraction versus q^2. Untagged measurements[28, 29, 30] can do so, and combined fits to data points and LQCD points as a function of q^2 provide the most precise determination of $|V_{ub}|$ from this mode. The world average[6] branching fraction for $\bar{B} \to \pi \ell \bar{\nu}$ is $(1.36 \pm 0.05 \pm 0.05) \times 10^{-4}$.

The lattice points entering the fit are calculated using 2+1 light quark flavors, and are provided in the region $q^2 > 16\,\mathrm{GeV}^2/c^4$. A combined fit to the most recent BABAR preliminary q^2 spectrum[30], parameterizing the form factor to order $O(z^2)$ (see Fig. 4) gives

$$|V_{ub}| = (2.95 \pm 0.31) \times 10^{-3} \tag{5.1}$$

where the uncertainty has comparable contributions from experiment and lattice. Determinations based on comparing partial rates at high q^2 with lattice calculations or at low q^2 with Light Cone Sum Rule calculations give somewhat larger values and larger uncertainties.

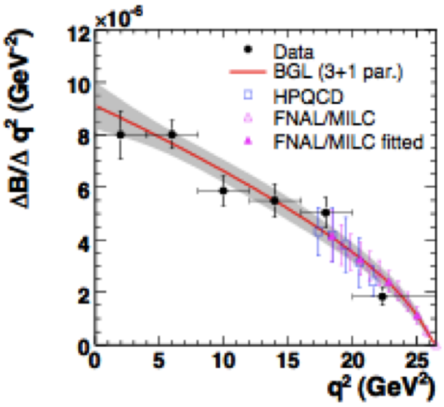

Figure 4: Combined fit to BABAR data and LQCD points to extract $|V_{ub}|$.

6. Summary and outlook

The $|V_{ub}|$ values obtained from the inclusive and exclusive determinations differ by 2.7σ. This trend has been seen for several years, and seems to persist despite improvements in precision and the confidence gained from additional, independent measurements and calculations. The most obvious potential sources of error in the inclusive result are in determinations of m_b, weak annihilation and perturbative corrections. The exclusive result relies heavily on the determination of the form factor normalization from LQCD.

The same trend is seen in $|V_{cb}|$ determinations, where the inclusive result is larger than the exclusive determinations by about 2.4σ.

The existing B factory data sets can still provide increased precision on experimental input, in particular on the $\bar{B} \to D\ell\bar{\nu}$ and $\bar{B} \to \pi\ell\bar{\nu}$ partial branching fractions and on inclusive $b \to u\ell\bar{\nu}$ partial rates.

References

[1] A.V. Manohar, M.B. Wise, Phys.Rev.**D49**:1310(1994); I.I. Bigi *et al.*, Phys.Rev.Lett.**71**:496(1993), Phys.Lett.**B323**:408(1994).

[2] CLEO, Phys.Rev.Lett.**89**:081803(2002); BELLE, arXiv:0810.1657; BABAR, Phys.Rev.**D77**:032002(2008).

[3] ALEPH, Phys.Lett.**B395**:373(1997); OPAL, Phys.Lett.**B482**:15(2000); DELPHI, Phys.Lett.**B510**:55(2001); DELPHI, Eur.Phys.J.**C33**:213(2004).

[4] BABAR, Phys.Rev.Lett.**100**:231803(2008).

[5] BABAR, Phys.Rev.**D79**:012002(2009).

[6] http://www.slac.stanford.edu/xorg/hfag/semi/fpcp2009/home.shtml.

[7] C. Bernard *et al.*, Phys.Rev.**D79**:014506(2009).

[8] BABAR, Phys.Rev.Lett.**104**:011802(2010).

[9] M. Okamoto *et al.*, Nucl.Phys.(Proc. Supp.)**B140**:461(2005); A. Kronfeld at CKM05 workshop, San Diego, CA, March 2005.

[10] D. Benson *et al.*, Nucl.Phys.**B665**:367(2003); P. Gambino, N. Uraltsev, Eur.Phys.J.**C34**:181(2004); D. Benson, I.I. Bigi, N. Uraltsev, Nucl.Phys.**B710**:371(2005).

[11] C.W. Bauer *et al.*, Phys.Rev.**D70**:094017(2004).

[12] I.I. Bigi *et al.*, Phys.Rev.**D52**:196(1995).

[13] BABAR, Phys.Rev.**D69**:111104(2004); BELLE, Phys. Rev. **D75**:32001(2007); DELPHI, Eur.Phys.J.**C45**:35(2006).

[14] BABAR, Phys.Rev.**D81**:032003(2010); BELLE, Phys.Rev.**D75**:032005(2007); CDF, Phys.Rev.**D71**:051103(2005); CLEO, Phys.Rev.**D70**:032002(2004).

[15] BABAR, Phys.Rev.**D72**:052004(2005); Phys.Rev.Lett.**97**:171803(2006); BELLE, Phys.Rev.Lett.**103**:241801(2009); CLEO, Phys.Rev.Lett.**87**:251807(2001).

[16] http://www.slac.stanford.edu/xorg/hfag/semi/EndOfYear09/gbl_fits/kinetic/index.html.

[17] Phillip Urquijo, private communication.

[18] CLEO, Phys.Rev.Lett.**88**:231803(2002).

[19] BABAR, Phys.Rev.Lett.**95**:111801(2005), ibid.**97**:019903(2006).

[20] BELLE, Phys.Lett.**B621**:28-40(2005).

[21] BABAR, Phys.Rev.**D73**:012006(2006).

[22] BELLE, Phys.Rev.Lett.**92**:101801(2004).

[23] BABAR, Phys. Rev. Lett.**100**, 171802 (2008).

[24] BELLE, Phys.Rev.Lett.**104**:021801(2010).

[25] C. Greub, M. Neubert, B.D. Pecjak, arXiv:0909.1609.

[26] BABAR, Phys.Rev.Lett.**101**:081801(2008); Phys.Rev.Lett.**97**:211801(2006).

[27] BELLE, Phys.Lett.**B648**:139(2007); arXiv:0812.1414.

[28] CLEO, Phys.Rev.Lett.**99**:041802(2007).

[29] BABAR, Phys.Rev.Lett.**98**:091801(2007).

[30] BABAR, arXiv:1005.3288.